Carbon formation thresholds and catalyst deactivation during CH_4 decomposition on supported Co and Ni catalysts

Yi Zhang and Kevin J. Smith*

Department of Chemical and Biological Engineering, University of British Columbia, 2216 Main Mall Vancouver, BC Canada, V6T 1Z4

Received 6 February 2004; accepted 10 March 2004

Carbon deposition during catalytic CH_4 decomposition ($CH_2 \leftrightarrow C + 2H_2$), occurs at a given reaction temperature when $K_M < K_M^*$, where K_M^* is the carbon formation threshold defined as the value of $K_M = (P_{H_2}^2/P_{CH_4})$ at which the net rate of carbon deposition is zero (Snoeck *et al.*, J. Catal. 169 (1997) 240). Carbon deposition can produce encapsulating carbon that results in catalyst deactivation, or filamentous carbon that ensures stable catalyst activity for extended periods of time. In the present study, the rate of catalyst deactivation during CH_4 decomposition at 773 K on supported Co and Ni catalysts decreased as K_M increased. A filamentous carbon formation threshold K_M^f is therefore defined as the value of K_M at which the rate of catalyst deactivation equals zero as a consequence of filamentous carbon formation. Results presented herein demonstrate that stable activity and filamentous carbon formation during CH_4 decomposition on supported Ni and Co catalysts can be guaranteed by choosing K_M such that the inequality $K_M^f < K_M < K_M^*$ is satisfied, whereas if $K_M < K_M^f < K_M^*$, encapsulating carbon accompanied by catalyst deactivation occurs.

KEY WORDS: carbon deposition; catalyst deactivation; methane decomposition; carbon formation threshold.

1. Introduction

Methane conversion to more valuable products is of interest because of the existence of large reserves of natural gas (> 80% CH_4 by volume), petroleum-associated gas, and methane hydrate [1,2]. Direct methane conversion by methane oxidative coupling, methane aromatization and methane homologation, or indirect methane conversion by conventional steam reforming, dry reforming and partial oxidation, are all described in the literature [3–7]. More recently, a cyclic process in which methane cracking is followed by gasification of carbon with steam or oxygen, in order to produce high purity hydrogen, has also been investigated [8,9].

In all of these CH_4 conversion processes, the activity of the catalyst for CH_4 activation and the carbon species formed during CH_4 decomposition are important, since both influence the life of the catalyst and the selectivity and yield to the desired products [5,6,10,11]. Previous studies of CH_4 decomposition on Co/SiO_2 catalysts at moderate temperatures showed that filamentous carbon was formed at specific reaction conditions and that the conditions required were similar to those required with Ni catalysts [12,13]. The mechanism of filament carbon formation, described in the literature [14], assumes that CH_4 decomposes on the catalyst metal surface according to the overall reaction $CH_4 \leftrightarrow C + 2H_2$, forming single carbon atoms. The carbon atoms dissolve in the metal and diffuse through the metal particle, although some surface diffusion around the outside of the particle may also occur [15]. The carbon precipitates in the form of graphite at the interface between the metal particle and the support and the metal particle is detached from the support by the formation of carbon filaments. The filaments grow and the metal surface remains active since the carbon deposited by CH_4 decomposition is removed from the surface by diffusion through the particle. The consequence of this mechanism is that stable CH_4 decomposition activity is observed for extended periods of time. Alternatively, the carbon deposited on the catalyst surface can encapsulate the metal particle, resulting in rapid catalyst deactivation [16,17]. In previous studies [12,13], stable catalyst activity or catalyst deactivation was observed depending on the catalyst, the catalyst properties and the operating conditions used during CH_4 decomposition.

An extended period of stable activity during CH_4 decomposition is critical for practical processes aimed at producing pure H_2 and nanofibre carbon. Carbon deposition during CH_4 decomposition depends on the operating conditions (T, P_{H_2}, P_{CH_4}) because H_2 evolution parallels CH_4 decomposition and the adsorption of H_2 onto the metal catalyst can promote gasification of deposited carbon species [18]. According to Snoeck *et al.* [14], the coking threshold defines those conditions at which there is no carbon deposition and no carbon gasification on the catalyst surface, i.e., the coking threshold corresponds to the conditions for which the rates of all consecutive steps of carbon formation are zero, $K_M^* = (P_{H_2}^2/P_{CH_4})_{r_c=0}$. Consequently, with

* To whom correspondence should be addressed.
E-mail: kjs@interchange.ubc.ca

1011-372X/04/0500–0007/0 © 2004 Plenum Publishing Corporation

$K_M = (P_{H_2}^2/P_{CH_4})$, carbon deposition will occur during CH_4 decomposition when $K_M < K_M^*$ whereas, when $K_M > K_M^*$, carbon gasification occurs. $K_M < K_M^*$ defines the reaction conditions (T, P_{H_2}, P_{CH_4}) under which carbon deposition is thermodynamically feasible, however, K_M^* does not determine whether filamentous or encapsulating carbon will be produced. Hence, K_M^* cannot be used to predict conditions that will ensure extended periods of stable catalyst activity associated with filamentous carbon formation during CH_4 decomposition.

In the present work, we present the concept of a filamentous carbon formation threshold, K_M^f that allows one to define the process conditions under which filamentous carbon formation will be observed during CH_4 decomposition on Ni and Co catalysts. By knowing K_M^* and K_M^f, the value of $K_M = (P_{H_2}^2/P_{CH_4})$ that will ensure stable catalyst activity can be determined.

2. Experimental

2.1. Catalyst preparation

Co catalysts were prepared by incipient wetness impregnation of a silica support using an aqueous solution of $Co(NO_3)_2 \cdot 6H_2O$ (+98%, Aldrich). Precalcined (25 h at 773 K) silica gel (grade 62, 60–200 mesh, 15A, Aldrich 24398-1) with a BET surface area of 300 m^2/g and pore volume of 1.15 mL/g was used as the support. The 5 wt%Ni catalyst was also prepared by incipient wetness impregnation of the support using an aqueous solution of $Ni(NO_3)_2 \cdot 6H_2O$ (+98%, Aldrich). The 2 wt%Ni catalysts was prepared similarly on a ZrO_2 support. After impregnation, the catalysts were dried at 383 K for 37 h and then calcined for 10 min at 723 K in static conditions at a ramp rate 10 K/min. Before being exposed to reactant, all catalysts (0.2 g) were reduced by temperature-programmed reduction (TPR) in a 100 mL/min 40%H_2/Ar to the desired temperature (table 1) in 1 h.

2.2. Catalyst characterization

Catalyst surface areas and pore volumes were measured by N_2 adsorption–desorption at 77 K using a FlowSorb II 2300 Micromeritics analyzer. A 30%N_2/He mixture was used for surface area measurement and a 95%N_2/He mixture fed at 20 mL/min was used for pore volume measurement. Samples were degassed at 398 K for approximately 3 h prior to measurement. The catalyst metal dispersion was determined by CO chemisorption. The CO uptake was measured gravimetrically (Perkin-Elmer TGS–2 thermogravimetric analyzer with a sensitivity of ± 1 μg) and procedural details have been provided previously [12]. The formation of filamentous carbon was detected by TEM (Hitachi H-800 electron microscope) examination of the used catalysts. Other experimental details have been provided elsewhere [12,13].

2.3. Catalyst activity and deactivation

The methane decomposition rate on the catalysts of interest was measured in a fixed-bed reactor operated isothermally in differential mode. Gas flow rates were controlled by calibrated Brooks 5878 mass flow controllers. The stainless steel reactor ($l = 60$ cm, o.d. = 0.95 cm) was loaded with 0.2 g catalyst (average particle size 0.17 mm) that was supported on a quartz wool plug. A thermocouple was placed close to the top of the catalyst bed to control the reaction temperature. A Varian Star 3400CX gas chromatograph, fitted with flame ionization and thermal conductivity detectors connected in series, and equipped with a 60/80 Carbosieve G column, was used for the product and feed gas analyses. UHP grade H_2, CH_4, He, Ar (99.999%,

Table 1
Properties of Co/SiO_2, Ni/SiO_2 and Ni/ZrO_2 catalysts of the present study

Metal loading (wt%)	BET SA (m^2/g)	PV (cc/g)	Redn. temp (K)	Redn. degree (mol%)	CO uptake (mmol/g)	Metal dispersion (%)	d_p (CO uptake) (nm)	d_p (TEM) (nm)	Max TOF[a] (L/min)
2 Ni[b]	45	0.205	923	100	0.031	9.2	10.5	–	0.4
5 Ni[c]	251	0.618	723	100	0.027	3.1	30.9	33.2	13.1
5 Co	239	0.971	923	100	0.084	9.2	10.4	–	1.0
8 Co	230	1.080	923	100	0.103	7.1	13.5	–	2.3
10 Co	217	0.989	923	100	0.094	5.4	17.8	–	3.9
12 Co	210	0.889	923	100	0.102	5.0	19.4	25[d]	3.7
30 Co	–	–	923	89.4	0.155	3.4	28.3	26[e]	6.1

d_p Estimated metal particle size; BET SA – surface area; PV – pore volume.
[a] Activity of catalysts shown in terms of maximum turnover frequency were measured at 773 K.
[b] Supported on ZrO_2.
[c] Supported on SiO_2.
[d] Estimated from TEM image of catalyst after reaction at 723 K.
[e] Measured from TEM image of catalyst after reaction at 773 K.

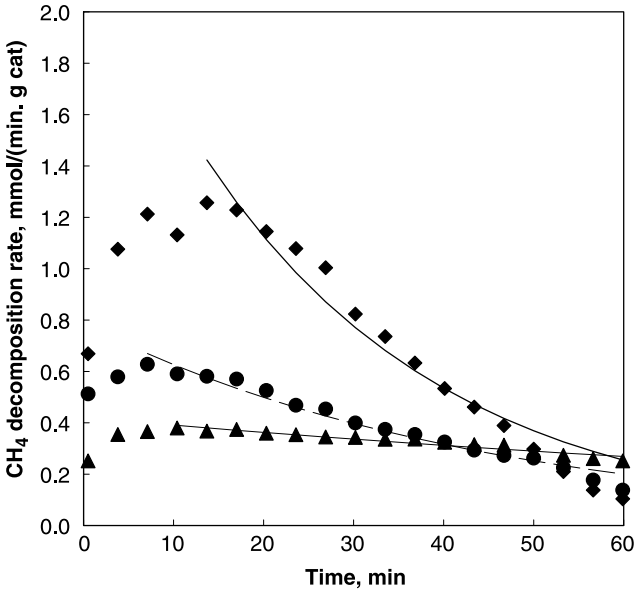

Figure 1. Activity of 12 wt%Co/SiO_2 catalysts, with different $K_M = P^2_{H_2}/P_{CH_4}$ ratios (Catalyst reduced at 923 K, reacted at 773 K, total gas flow 185 mL/min, weight of catalyst = 0.2 g; Solid lines are the fit of equation (1) to the experimental data points; (◆) $K_M = 0.01$ atm; (●) $K_M = 0.03$ atm; (▲) $K_M = 0.05$ atm).

Praxair), 5%CH_4/Ar calibrated gas (Praxair) were used in the experiments. For the range of experimental conditions used in the present study, internal and external gradients in concentration and temperature were insignificant [19].

Figure 1 shows typical curves of the measured CH_4 decomposition rate versus time for Co catalyst in the presence of a H_2/CH_4 feed. The activity profiles for CH_4 decomposition were of similar form for all the catalysts investigated herein. The CH_4 decomposition rate first increases to a maximum, then decreases. The activity profiles are conveniently described by a kinetic equation of the type $r = r^* a$, where r^* is the maximum decomposition rate and a is the catalyst activity factor [16]. If the time corresponding to the maximum is designated t^*, and if the rate is 1st order with respect to the activity factor, i.e. $da/dt = -k_d a^d$, where $d = 1$ and k_d is the decay constant, the methane decomposition kinetics after the maximum can be described by equation (1):

$$r = r^* e^{-k_d(t-t^*)} \quad (1)$$

Curve fitting the decomposition rate data after the maximum rate versus $(t - t^*)$ using Table 2D curve software (SPSS Inc.), as shown in figure 1, provided estimates of r^* and k_d. These two parameters are conveniently used to discuss the catalyst maximum activity (r^*) and deactivation rate, k_d, throughout the present study. For all of the data reported herein, the fits to the 1st order decay model had regression coefficients $R^2 > 0.90$.

In the present study, both decreasing activity ($k_d > 0$) and stable activity ($k_d = 0$) were observed on supported Co and Ni catalysts. The maximum activity in the case of declining activity was determined by the method described above. The maximum activity in the case of stable activity was estimated directly from the measured data.

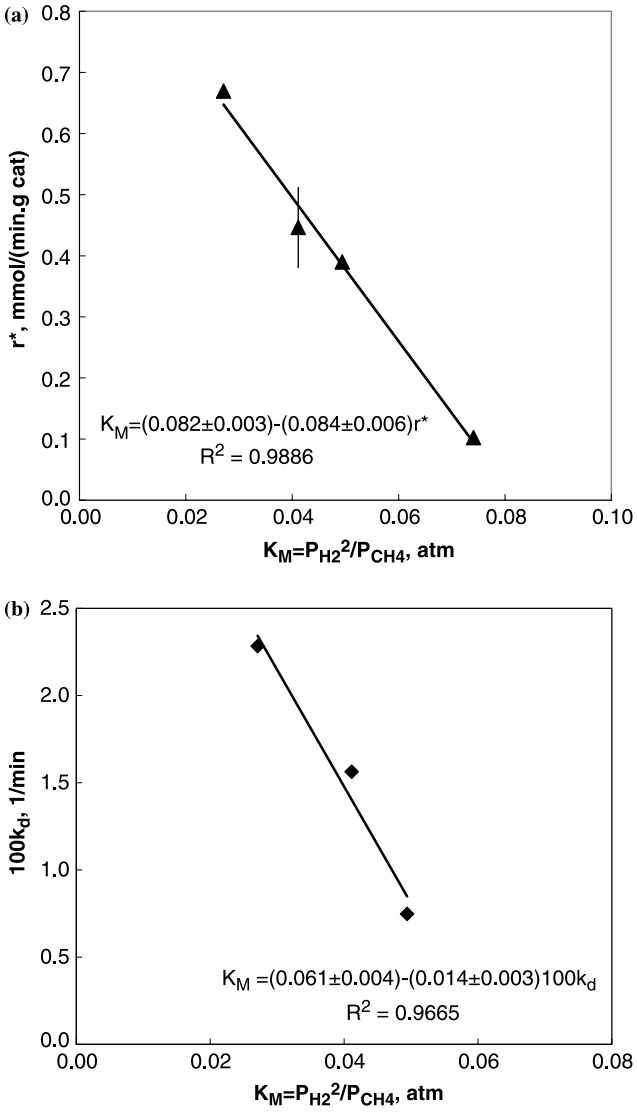

Figure 2. (a) Dependence of maximum rate r^* on K_M with 12 wt%Co/SiO_2 at 773 K ($K^*_M = 0.082 \pm 0.003$ atm). (b) Dependence of deactivation rate 100 k_d on K_M with 12 wt%Co/SiO_2 at 773 K ($K^f_M = 0.061 \pm 0.004$ atm).

3. Results

A series of Co/SiO_2 catalysts (table 1) with estimated metal particle size (d_p) in the range 10–28 nm were obtained by reducing 5–30 wt%Co/SiO_2 at 923 K. Properties of the Ni/SiO_2 catalyst are also reported in table 1. Note that for the SiO_2 supported catalysts with the same metal loading, $d_{p,Co} < d_{p,Ni}$. As noted in previous studies [12,13], larger metal particles favor filament formation and hence stable activity is most often observed on Ni catalysts.

The CH_4 decomposition activity profiles were the focus of the present study and these were determined for the 12wt%Co and 5 wt%Ni catalysts at 773 K while varying the value of $K_M = P_{H_2}^2/P_{CH_4}$ from 0.01 to 0.10 atm. At each operating condition, the maximum TOF (maximum TOF = r^*/the number of active sites) and the decay constant ($100\,k_d$) were estimated by fitting the experimental data to the 1st order decay model, as described in the section 2. The values obtained at 773 K for the Co and Ni catalysts are presented in figures 2 and 3. Clearly the ratio $K_M = P_{H_2}^2/P_{CH_4}$ had a significant effect on the catalyst activity and deactivation: both catalyst activity, r^* and deactivation rate, k_d decreased with increasing K_M at 773 K on the 12 wt%Co/SiO_2 catalyst and on the 5 wt%Ni/SiO_2 catalyst.

The point at which the CH_4 decomposition activity is zero, estimated by drawing a trendline through the data of figure 2a, corresponds to the coking threshold, $K_M^* = (P_{H_2}^2/P_{CH_4})_{r^*\to 0}$. The coking threshold defines those conditions at which there is no carbon deposition and no carbon gasification on the catalyst surface [14]. When $K_M < K_M^*$, CH_4 decomposition with carbon deposition will occur, whereas when $K_M > K_M^*$, carbon gasification occurs.

Similarly, figure 2b shows that 100 k_d approached zero with increasing K_M. The point at which 100 k_d equals zero, obtained by drawing a trendline through the data of figure 2b, is defined herein as the filamentous carbon formation threshold, $K_M^f = (P_{H_2}^2/P_{CH_4})_{k_d\to 0}$. The filamentous carbon formation threshold, K_M^f proposed by analogy to the coking threshold K_M^*, is based on the observation that stable activity during CH_4 decomposition corresponds to filamentous carbon formation [12–14]. Figures 2b and 3b show that 100 k_d decreased with increasing K_M. When the value of $K_M > K_M^f$, filamentous carbon is produced and stable catalyst activity will be observed ($k_d = 0$), whereas, when $K_M < K_M^f$, encapsulating carbon is produced and deactivation occurs ($k_d > 0$).

An extended period of stable activity during CH_4 decomposition is critical for practical processes aimed at producing pure H_2 and nanofibre carbon. The two thresholds K_M^* and K_M^f can be used to predict the operating conditions (i.e. the value of K_M) needed for stable activity during CH_4 decomposition on certain catalysts, especially low loading metal catalysts at fixed temperature. Stable activity with carbon deposition would occur during CH_4 decomposition when filamentous carbon is produced, and filamentous carbon is formed when K_M satisfies the condition: $K_M^f < K_M < K_M^*$. Figure 2 shows that on 12 wt%Co/SiO_2 catalyst at 773 K, $K_M^* = 0.082 \pm 0.003$ atm and $K_M^f = 0.061 \pm 0.004$ atm. Hence, K_M must satisfy the condition: $0.061 \pm 0.004 = K_M^f < K_M < K_M^* = 0.082 \pm 0.003$ atm, for stable activity during CH_4 decomposition. Figure 4 shows that stable activity was indeed obtained when $K_M = 0.074$ atm on the same catalyst at 773 K.

Stable activity during CH_4 decomposition is often reported on high loading Ni catalysts [20], but deactivation has been observed on low loading Ni catalysts, (5 wt% Ni/SiO_2) in the present study. The dependence of r^* and k_d on K_M is presented in figure 3a and b as determined for the 5 wt%Ni/SiO_2 catalyst at 773 K. K_M^* and K_M^f were obtained from figure 3a and b, respectively. Hence, $K_M^* = 0.110 \pm 0.009$ atm and $K_M^f = 0.032 \pm 0.003$ atm. Consequently, K_M must satisfy the condition: $0.032 \pm 0.003 = K_M^f < K_M < K_M^* = 0.110 \pm 0.009$ atm for stable activity to be observed during CH_4 decomposition on 5 wt%Ni/SiO_2 at 773 K. Figure 4 shows that indeed stable activity was obtained when $K_M = 0.09$ atm for the 5 wt%Ni/SiO_2 catalyst at 773 K. The results presented in figure 4 show that stable activity can be obtained provided K_M is chosen such that $K_M^f < K_M < K_M^*$.

3.1. Effect of metal particle size on thresholds

The effect of metal particle size on coking threshold, K_M^* has been described by Rostrup-Nielsen [21]. Accordingly, the difference in the Gibbs free energy change between filamentous carbon and graphitic carbon ($CH_4 \rightarrow C_{graphite} + 2H_2$) formation from CH_4 (or CO) decomposition can be expressed by equations (2) and (3) in terms of the equilibrium constant [21,22].

$$\Delta G_c = \Delta G^0_{observed} - \Delta G^0_{graphite} \tag{2}$$

$$\Delta G_c = -RT \ln\left(\frac{K_{observed}}{K_{graphite}}\right) \tag{3}$$

Rostrup-Nielsen [21] reported that deviations from graphite equilibrium for CO and CH_4 decomposition, on a large number of Ni catalysts, can be explained by the extra energy required by the surface and defect structure of the filaments, as expressed by equation (4).

$$\Delta G_c = \mu - \mu_0 + \mu^* \tag{4}$$

The term $\mu - \mu_0$ corresponds to the extra surface energy due to the cylindrical form of the filament. The term μ^* corresponds to the extra energy from surface defects. A simple Kelvin equation can be used to determine ΔG_c, as shown in equation (5):

$$\Delta G_c = 2(\gamma^* M/\rho_c) * (1/d_p) + \mu^* \tag{5}$$

Equation (5) shows that the surface energy increases with decreasing metal particle size. According to equation (5), by linear regression of ΔG_c versus $1/d_p$, γ, the surface tension of the carbon fibres, and μ^*, the defect contribution, can be estimated from the obtained slope and intercept, knowing the molecular mass (M) and density (ρ_c) of graphitic carbon.

In the present study, ΔG_c on different Co and Ni catalysts was calculated from the experimental values of K_M^* and $K_{graphite} = 0.462$ atm at 773 K [21] using equation (3). The obtained values of ΔG_c are plotted versus the

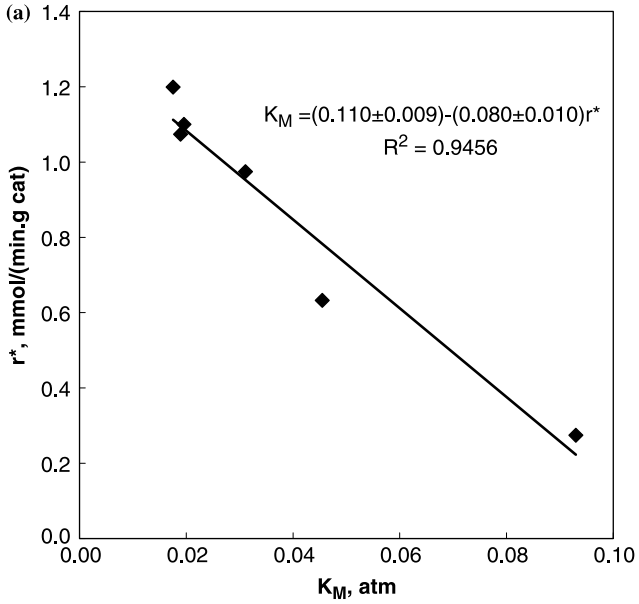

Figure 3. (a) Dependence of maximum rate r^* on K_M with 5 wt%Ni/SiO_2 at 773 K ($K_M^* = 0.110 \pm 0.009$ atm). (b) Dependence of deactivation rate 100 k_d on K_M with 5 wt%Ni/SiO_2 at 773 K ($K_M^f = 0.032 \pm 0.003$ atm).

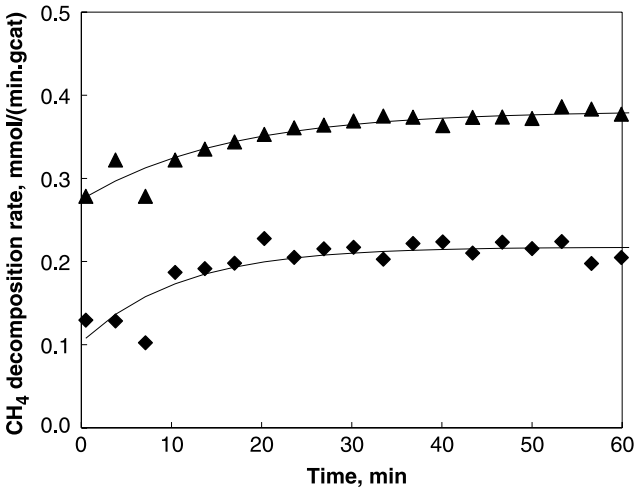

Figure 4. Stable activities were obtained when K_M satisfies the inequality $K_M^f < K_M < K_M^*$ (◆) 12 wt%Co/SiO_2 with $K_M = 0.074$ atm at 773 K; (▲) 5 wt%Ni/SiO_2 with $K_M = 0.09$ atm at 773 K).

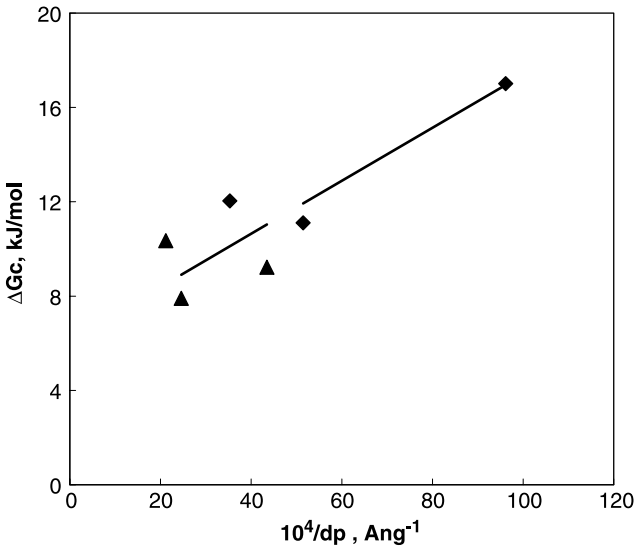

Figure 5. Deviation of the coking threshold from graphite equilibrium and the effect of metal crystallite size during CH_4 decomposition on Ni and Co catalysts at 773 K. (◆) Co/SiO_2; (▲) Ni/SiO_2; $\Delta G_c = 0.101(10^4/d_p) + 6.68$.

reciprocal of the average metal particle size in figure 5. The data of figure 5 show a linear relationship as described by equation (5). The intercept and slope of the data of figure 5 provided an estimated surface tension of $\gamma = 8.4$ J/m^2 and a defect contribution to ΔG_c of approximately $\mu^* = 6.7$ kJ/mol at 773 K, assuming the density of filamentous carbon is equal to 2.0 g/mL. The value of the surface tension is comparable to the surface tensions of about 7.9 and 7.4 J/m^2 at 773 K reported for the CO–CO_2 and CH_4–H_2 equilibria, respectively [21]; the defect contribution of 6.7 kJ/mol is comparable to values of 8.4 and 2.9 kJ/mol at 773 K for the CO–CO_2 and CH_4–H_2 equilibria, respectively [21]. The results from the present study confirm that the deviation in K_M^* from the value expected for graphite can be explained by a more disordered structure of the carbon, and by a contribution from the surface energy of the carbon filament [21]. The metal type (Ni or Co catalyst) appeared to have no influence on the observed equilibrium.

On Co/SiO_2 catalysts with different Co loading, K_M^f and K_M^* were obtained as before and the difference between the coking threshold and filamentous carbon threshold, $(K_M^* - K_M^f)$, is plotted versus metal particle size in figure 6. The data show that the difference between the coking threshold and filamentous carbon formation threshold increases with increasing Co particle size. Stable catalyst activity with carbon deposition during CH_4 decomposition occurs when K_M satisfies the inequality $K_M^f < K_M < K_M^*$. It follows, therefore, that an

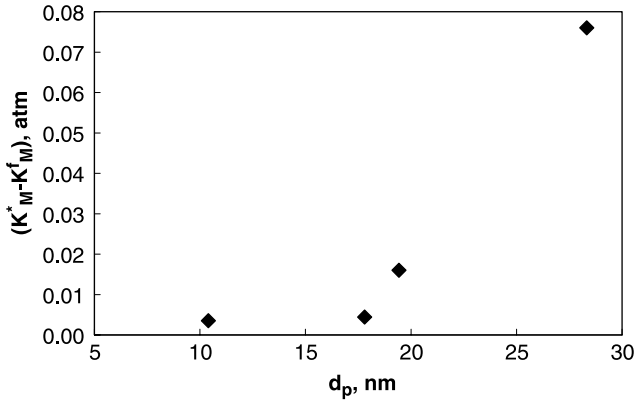

Figure 6. The difference between the coking threshold and the filamentous carbon formation threshold, $(K^*_M - K^f_M)$ at 773 K with increasing Co particle size.

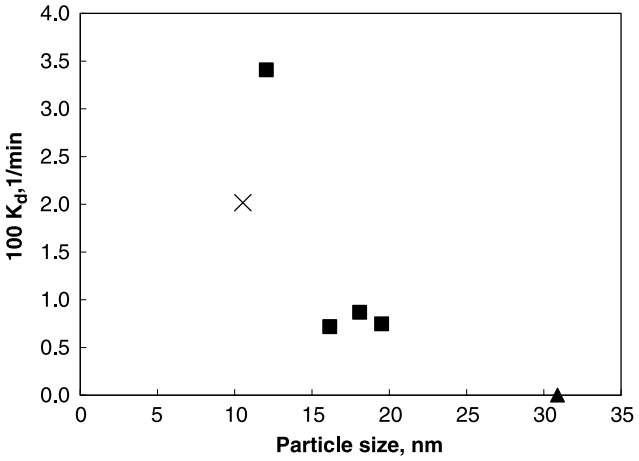

Figure 7. Dependence of the catalyst deactivation rate $(100k_d)$ on metal particle size at 773 K with $K_M = 0.06$ atm (■) Co/SiO_2; (▲) Ni/SiO_2; (×) Ni/ZrO_2).

increasing difference between K^f_M and K^*_M with increasing metal particle size, increases the window of suitable operating conditions (K_M) for stable catalyst activity and filamentous carbon formation. This is also consistent with the data of figure 7 showing that at the same K_M, stable activity with filamentous carbon formation was obtained on larger metal particles ($k_d \to 0$ as d_p increased).

4. Conclusions

A filamentous carbon formation threshold K^f_M is defined as the value of $K_M = (P^2_{H_2}/P_{CH_4}) < K^*_M$ that corresponds to stable catalyst activity ($k_d \to 0$) during CH_4 decomposition on supported Ni and Co catalysts. Stable catalyst activity is observed as a consequence of filamentous carbon formation. Conditions for stable activity during CH_4 decomposition on supported Ni and Co catalysts are defined by K_M that satisfies the inequality $K^f_M < K_M < K^*_M$.

Acknowledgments

Funding for the present study form the Natural Sciences and Engineering Research Council of Canada is gratefully acknowledged.

References

[1] C. Gueret, M. Daroux and F. Billaud, Chem. Eng. Sci. 52 (1997) 815.
[2] B. Gaudernack and S. Lynum, Int. J. Hydrogen Energy 23 (1998) 1087.
[3] A.M. Maitra, Appl. Catal. A-Gen. 104 (1993) 11.
[4] T. Koerts and R.A. van Santen, J. Chem. Soc. Chem. Commun. (1991) 1281.
[5] Y.D. Xu and L.W. Lin, Appl. Catal. A-Gen. 188 (1999) 53.
[6] M.A. Pena, J.P. Gomez and J.L.G. Fierro, Appl. Catal. A-Gen. 144 (1996) 7.
[7] H. Jiang, L.S. Wang, W. Cui and Y.D. Xu, Catal. Lett. 57 (1999) 95.
[8] T.J. Zhang and M.D. Amiridis, Appl. Catal. A-Gen. 167 (2) (1998) 161.
[9] T.V. Choudhary and D.W. Goodman, J. Catal. 192 (2000) 316.
[10] J.Z. Luo, Z.L. Yu, C.F. Ng and C.T. Au, J. Catal. 194 (2000) 198.
[11] H. Amariglio, J. Saint Just and A. Amariglio, Fuel Process. Tech. 42 (1995) 291.
[12] Y. Zhang and K.J. Smith, Catal. Today 77 (2002) 257.
[13] Y. Zhang and K.J. Smith, Appl. Catal. A-Gen., in press.
[14] J.-W. Snoeck, G.F. Froment and M. Fowles, J. Catal. 169 (1997) 240.
[15] V.L. Kuznetsov, A.N. Usoltseva and A.L. Chuvilin, Phys. Rev. B 64 (2001) 235401.
[16] M.C. Demicheli, E.N. Ponzi, O.A. Ferretti and A.A. Yeramian, Chem. Eng. Sci. 46 (1991) 129.
[17] G.G. Kuvshinov, Y.I. Mogilnykh and D.G. Kuvshinov, Catal. Today 42(3) (1998) 357.
[18] P.E. Nolan, M.J. Schabel, D.C. Lynch and A.H. Cutler, Carbon 33(1) (1995) 79.
[19] Y. Zhang, Thesis, Methane Decomposition Kinetics on Supported Co and Ni Catalysts, University of British Columbia, 2004.
[20] S.K. Shaikhutdinov, L.B. Avdeeva, O.V. Goncharova, D.I. Kochubey and B.N. Novgorodov, Appl. Catal. A-Gen. 126(1) (1995) 125.
[21] J.R. Rostrup-Nielsen, J. Catal. 27 (1972) 343.
[22] I. Alstrup, J. Catal. 109(2) (1988) 241.